Journal of Bio- and Tribo-Corrosion (2021) 7:36
https://doi.org/10.1007/s40735-020-00469-1

Comparative Analysis of Response Surface Methodology and Artificial Neural Network on the Wear Properties of Surface Composite Fabricated by Friction Stir Processing

Lakshay Tyagi[1] · Ravi Butola[1] · Luckshaya Kem[1] · Ranganath M. Singari[1]

Received: 26 July 2020 / Revised: 8 December 2020 / Accepted: 23 December 2020 / Published online: 23 January 2021

Abstract
Aluminium surface composite having ceramic reinforcement is successfully developed using friction stir processing at different tool rpm. Pin-on-disc test was performed at different sliding distances (300 m, 600 m, 900 m) and at different applied loads (20 N, 30 N, 40 N), to analyse wear behaviour of the fabricated composites. Response surface methodology (RSM) and Artificial neural network (ANN) are used to successfully develop two different models and a comparative study was done of the predictive capacity of both the developed models. The comparative study shows that the predictive capacity of the ANN model is more efficient than the RSM model. RSM is also utilized to optimize the process parameter. Optimum condition predicted by the model is for the composite developed at 1200 tool rotational speed, applied with a load of 20 N for a sliding distance of 300 m. Scanning electron microscopy (SEM) and Energy dispersive spectroscopy (EDS) analysis of wear surface were done, revealing that adhesive wear is the major wear mechanism and oxide layer formation is present on the wear surface.

Keywords Surface composite · Wear · Friction stir processing · Response surface methodology · Artificial neural network

1 Introduction

Aluminium is one of the widely available material in the earth's crust and has wide applications. It possesses properties like high strength, high toughness, and due to these characteristics it is preferred in the aerospace and automobile sectors [1–5]. Aluminium metal matrix composites (AMMC) are occupying great interest in industrial and manufacturing sectors due to its excellent properties like ductility, high strength, toughness, etc. [6]. Addition of reinforcement to matrix material enhances its mechanical and tribological properties. Some reinforcements like alumina (Al_2O_3), Boron carbide (B_4C), Silica (SiO_2), Silicon Carbide (SiC), Graphite (Gr), Tungsten carbide (WC) [7], and yttrium oxide are used to enhance the properties of the matrix material [8–10]. Various modelling and optimization techniques are being used nowadays in order to reduce the number of experiments performed and costs related to it. One of this type of modelling and optimization technique is Artificial neural network (ANN) [11]. ANN is the development of artificial intelligence to predict the behaviour of any material or a system [12, 13]. Various modelling and optimization techniques are being used nowadays in order to reduce the number of experiments performed and costs related to it. Pramod et al. [14] studied Al7075-Al_2O_3 composite and observed the wear behaviour, and analysed it using ANN. It was found that wear resistance improved in AA7075 reinforced with Al_2O_3. They also concluded that ANN is capable of predicting the wear loss. Atrian et al. [15] reinforced AA7075 with the nanoparticle of SiC and analysed ultimate tensile strength using neural network techniques like the stimulation of indentation test. Enhancement of about 300% was observed in ultimate tensile strength value. Mahanta et al. [16] reinforced Al7075 with 1.5wt% B_4C and (0.5, 1.0, 1.5wt%) fly ash using the ultrasonic stir casting method. Scanning electron microscope (SEM) analysis revealed that oxidation and abrasion are the main constituents of wear. Kumar et al. [17] used response surface methodology (RSM) to study AA7075 and aluminium hybrid metal matrix composite. They concluded

✉ Ravi Butola
ravibutola33855@gmail.com

[1] Mechanical Engineering Department, Delhi Technological University, New Delhi 110042, India

that wear rate decreases on increasing the transition speed and also specific wear rate for hybrid composite decreases on increasing the sliding distance. Response surface model gave error around 7% which is quite low. Dehghani et al. [18] optimized the bake hardening behaviour of Al7075 by using response surface methodology. They found that there is a good accord between the results predicted and found experimentally and also response surface methodology (RSM) provides high accuracy. Subramanian et al. [19] analysed the surface roughness of Al7075-T6 by using response surface methodology. It was observed that surface roughness increased exponentially concerning cutting feed rate, and surface roughness also increased with the decreasing cutting speed. Sivasankaran et al. [20] analysed the sliding behaviour of Al7075 with TiB_2/Gr reinforcement by using RSM. It was found that reinforcement content, load, sliding distance, sliding velocity, are the factors that effect wear rate of the material. Vishwakarma et al. [21] using RSM did the modelling of ageing parameters of coefficient of thermal expansion and thermal conductivity of AA6082. It was observed that ageing temperature is the ruling factor of both ageing factors taken into consideration. They discovered that thermal properties improved by ageing treatment, increasing the applications of Al6082 alloy. Coyal et al. [22] studied mechanical and tribological properties of AMMC reinforced with SiC and Jute ash. They found that on the addition of reinforcement tensile strength and microhardness of alloy increases. With the increasing content of reinforcement wear rate of the composite decreases. Parikh et al. [23] observed the wear behaviour of cotton fibre polyester composites and modelling was done using ANN. The results show that proper wt% can control the wear rate of material and it was found that ANN is the best tool to forecast the materials' wear behaviour. Abdelbary et al. [24] used pre-cracked nylon 66 and observed the effect of load frequency on wear properties and also by using ANN prediction of wear rate of pre-cracked Nylon 66. It was found that single transverse crack can be responsible for increasing the wear rate and ANN is effective in the prediction of wear rate. Merayo et al. [25] developed an ANN model for ultimate tensile strength and yield strength of aluminium alloys taking chemical composition, tempers, and hardness as input. They concluded that AI-based techniques can be used for prediction of tensile properties.

This study deals with the prediction and optimization of tribological properties of AMMC fabricated using friction stir processing (FSP). FSP contributes to the production of finer grains and enhanced mechanical properties with low production cost and in less time [26, 27]. Materials fabricated via FSP comprise reduced distortion and defects, compared to materials produced with other manufacturing processes [28]. AA7075 is reinforced with SiC as reinforcement and two models are developed, one using RSM and one with ANN methodology. In ANN, better model can be generated with fewer data points [29]. An attempt is made to conduct a comparative analysis of the predictive efficiency of the developed models. Morphology of the worn surface was done using SEM.

2 Experimental Procedure

2.1 Materials and Method

AMMC is developed taking AA7075 as matrix material, SEM image of the base material is shown in Fig. 1. The process like FSP can be easily performed on materials like aluminium [30]. Two lines having 50 holes each, each hole has a diameter of 2 mm and depth 3.5 mm, were drilled using CNC vertical milling machine on the centre of the base material. SiC powder having a particle size of around 40 µm was used as reinforcement and was filled in these holes in order to fabricate the surface composite.

Surface composites are prepared using friction stir processing. The composites fabricated have SiC (2 wt%) and are processed at three different FSP tool rotational speeds, i.e. 600, 900, and 1200 rpm. The tool which is used for processing is made of H13 tool steel, having a square tip with a tip length of 3.5 mm and a total length of 117 mm [31, 32]. The square tip was used in order to minimize the number of defects and distribute reinforcement uniformly [33]. Minimal defects and uniform distribution in composite fabricated with square pin tool are due to high amount of pulsation generated [34]. To fabricate the surface composite, first capping pass was done with a pinless tool to cover the holes filled with reinforcement powder. This is done to protect the loss of reinforcement from the holes during FSP tool pass. After the capping pass, FSP is carried out distributing reinforcement throughout the matrix

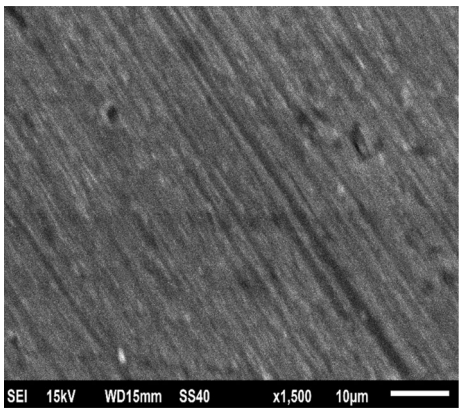

Fig. 1 SEM image of base material

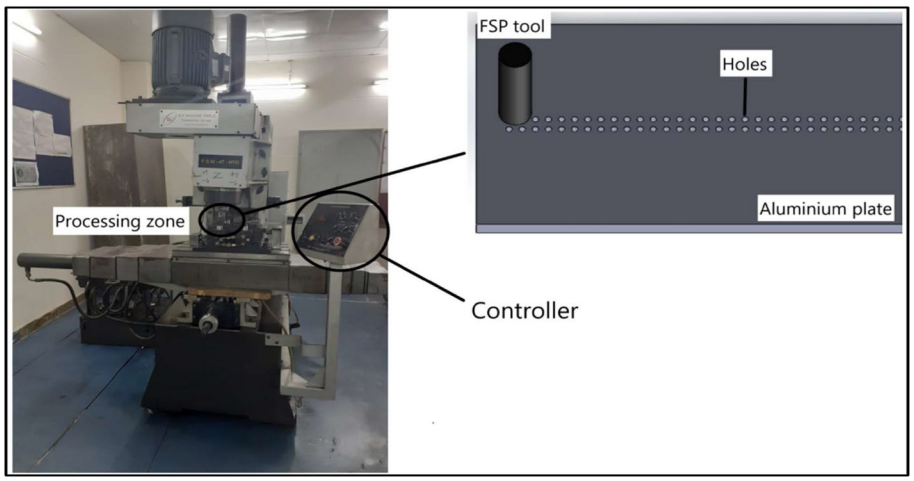

Fig. 2 Friction stir processing setup

Table 1 Process parameters of FSP

Process parameters	Value taken
Tool shoulder	Flat
Tool shoulder Dia	19.95 mm
Tool pin profile	Square
Tool pin length	3.5 mm
Tilt angle (degree)	2° constant
Tool rotational speed (rpm)	600, 900, 1200

uniformly. FSP setup and Process parameters are shown in Fig. 2 and Table 1.

2.2 Wear Experimentation

AA7075/SiC surface composites are prepared using FSP at different tool rotational speeds (rpm), and are used as specimens for wear tests. The test is carried out as per ASTM G99-04 standards. Specimens cylindrical in shape of diameter 10 mm and length 6 mm are carved out of the fabricated surface composite. The test is carried out on DUCOM manufactured; the schematic representation of high-temperature rotatory tribometer is shown in Fig. 3. In this test, the specimens are held and slid against a disc under the action of specific applied load. The disc against which the specimens are slid is made up of EN24 steel, having a hardness of 58 HRC. As a result of the experiment the parameters like wear, frictional force are acquired. The linear wear is monitored via Linear variable differential transducer (LVDT) assembly. The test is carried out at three different applied loads, i.e. 20 N, 30 N, 40 N and for a sliding distance of 300 m, 600 m, 900 m. All the experiments are carried out according to the developed design of experiment, and are discussed in the following sections.

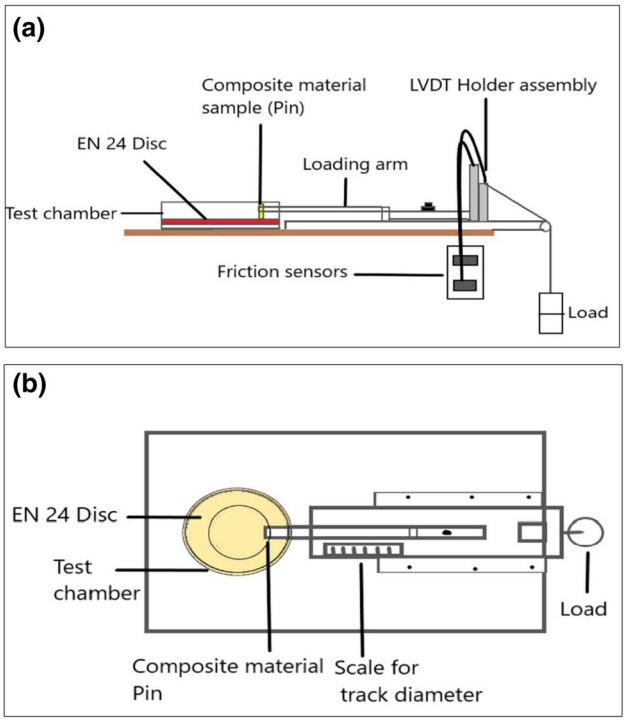

Fig. 3 Schematic representation of High-temperature rotatory tribometer **a** side view **b** top view

2.3 Development of Mathematical Models Using RSM

Performing experiments, the number of times in order to get better results is a very time-consuming and costly process [35]. To overcome this problem, response surface method is used. RSM develops a mathematical model based on the input data. Generally, a second-order mathematical model is generated. For a model having three factors, i.e. X1, X2, and X3 the equation is given as follows:

Table 2 Factors and their level for design of experiment

Levels	X1 (Tool rpm)	X2 (Sliding distance)	X3 (Load)
Level 1	600	300	20
Level 2	900	600	30
Level 3	1200	900	40

Table 3 Experimental design in coded values

Std	Run	X1	X2	X3
1	1	1	1	2
6	2	3	2	1
11	3	2	1	3
13	4	2	2	2
10	5	2	3	1
19	6	2	2	2
7	7	1	2	3
18	8	2	2	2
17	9	2	2	2
4	10	3	3	2
16	11	2	2	2
3	12	1	3	2
20	13	2	2	2
15	14	2	2	2
9	15	2	1	1
14	16	2	2	2
12	17	2	3	3
2	18	3	1	2
8	19	3	2	3
5	20	1	2	1

$$Y = a + a1\ \ X1 + a2\ \ X2 + a3\ \ X3 + a4\ \ X1 * X1 + a5\ X2 * X2 + a6\ \ X3 * X3 + a7\ \ X1 * X2 + a8\ \ X1 * X3 + a9\ X2 * X3.$$

Analysis of variance (ANOVA) is used to analyse the interaction of process parameters with the response. The F value signifies the statistical significance of the model. The probability value (P value) provides a base to evaluate the significant model terms, the confidence level of 95% or more works well. Adjusted mean square (Adj MS) measures how much variable a term or model explains and Adjusted sum of squares (Adj SS) explains the variation of different parts of the model. R^2 coefficient determines the accuracy of the fitted polynomial model [36]. For this study, modelling of data and experiment runs is done using Design Expert software. Box–Behnken design is used to generate 20 experimental runs for three factors having 3 levels each, and is shown in Table 2. The factors considered are FSP tool rpm (X1), sliding distance (X2), and applied load (X3). The generated experimental design generated by the software is shown in Table 3 In coded values.

2.4 Artificial Neural Network (ANN)

Artificial Neural Network (ANN) is widely used for forecasting purposes. It assigns weights to all the provided input factors based on the data. On the basis of these weights assigned to each factor, the prediction is done. Its greatest advantage is that it can model complex nonlinear and multidimensional relations without any prior assumptions [24]. Self-organizing capability helps in developing a network purely from experimental data [37]. ANN is a network of neurons which are interconnected to each other. Similarly, like neurons present in the human body they learn to adapt to inputs [16]. ANN consists of input layers, output layers, and hidden layers. Data are collected by the input layer and via hidden layers, it gets transmitted to the output layer [11]. During this process, different weights are assigned to each input factors according to their function. ANN is mainly used for nonlinear statistical data modelling. ANN comprises two phases, 1. Training Phase and 2. Testing Phase. Input data are divided into two parts one used for training the data and other part is used for testing of the trained model.

3 Results and Discussion

3.1 Wear

In Figs. 4 and 5, wear and coefficient of friction are shown as a function of sliding distance at different applied loads. It can be observed from both the figures that wear and coefficient of friction increase with increasing value of sliding distance and applied load. This increase due to increase in load can be attributed to delamination wear and increase in applied pressure [38–42]. As at lower loads, there is low pressure between the mating surfaces and at higher loads, this pressure between the mating surfaces is high and increased wear is observed. With wear, the matrix area gets removed from the surface and produced debris, giving rise to higher abrasion resulting in higher wear loss [43]. It can also be observed that wear for composite fabricated at higher tool rpm is less as compared to the composite processed at lower rpm. This is because the number of cavities and defects are reduced on fabricating a composite at higher rpm, making matrix more uniform and hence reducing wear [44]. Similar types of results are reported by Alam et al. when they studied wear behaviour of A356 reinforced with SiCn [9].

3.2 Response Surface Modelling and Optimization

Minitab Software package is used for developing RSM models for coefficient of friction and wear. Tables 4 and 5 show the analysis of variance results for wear and coefficient of friction, respectively. Regression model equation for wear

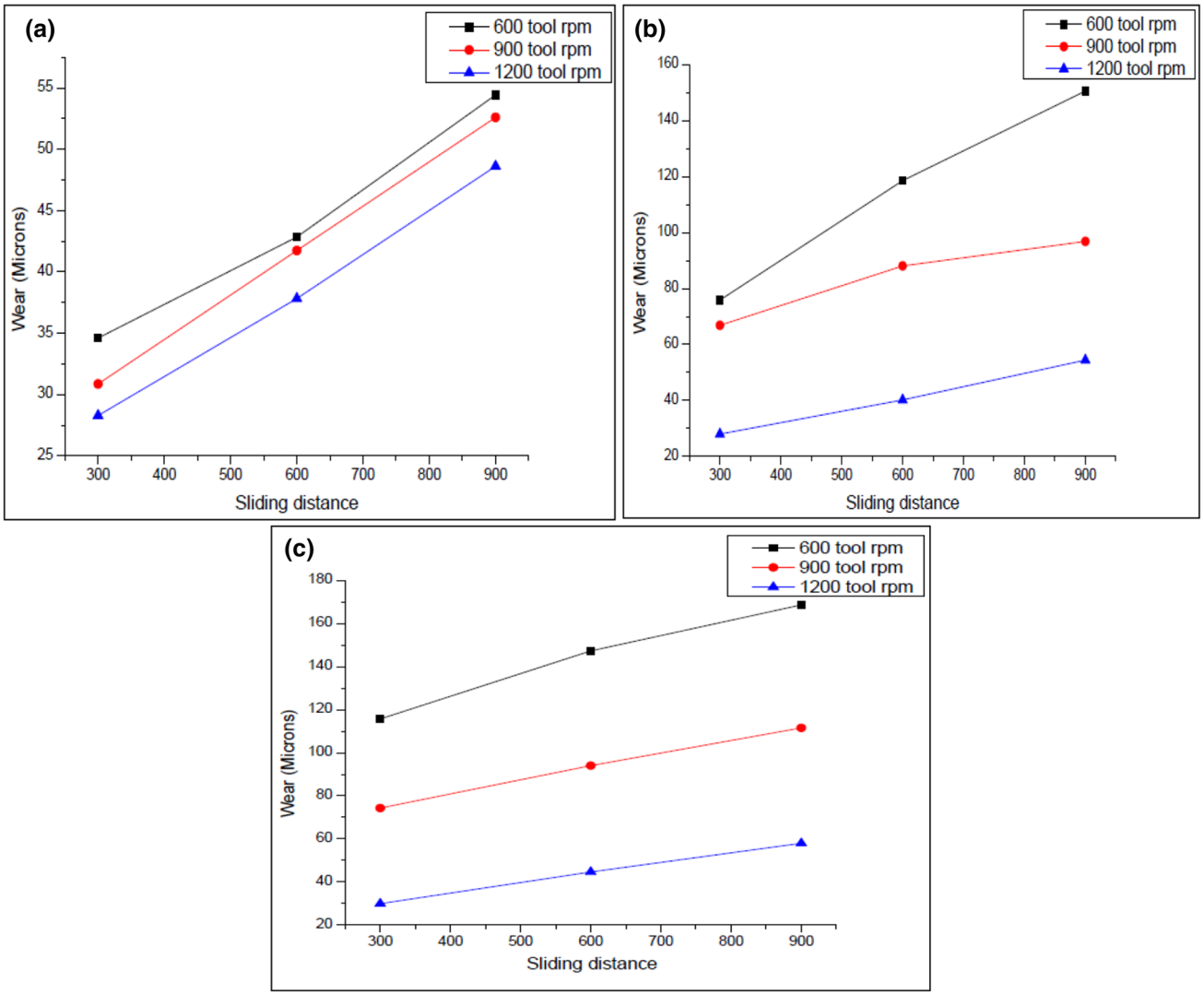

Fig. 4 Wear vs sliding distance at **a** 20 N applied load, **b** 30 N applied load, and **c** 40 N applied load

and coefficient of friction in coded factors is given in Eq. 1 and 2.

$$\begin{aligned}\text{Wear} = &-405.9 + 0.3167\,X1 + 0.2243\,X2 + 18.06\,X3 \\ &- 0.000054\,X1 \times X1 - 0.000063\,X2 \times X2 \\ &- 0.1473\,X3 \times X3 - 0000134\,X1 \times X2 \\ &- 0.00814\,X1 \times X3 + 0.00129\,X2 \times X3\end{aligned}$$

$$\begin{aligned}\text{Coefficient of friction} = &\ 0.331 + 0.000098\,X1 \\ &+ 0.000166\,X2 - 0.00971\,X3 - 0.0000\,X1 \times X1 \\ &- 0.000\,X2 \times X2 + 0.000154\,X3 \times X3 \\ &+ 0.0000X1 \times X2 + 0.000005X1 \times X3 \\ &- 0.000001\,X2 \times X3\end{aligned}$$

The F value for the wear model is 59.59 and the corresponding P value is 0.000, similar values can be seen in Table 4, it thus concludes that the developed model obtained is significant. For the model, the R^2 value obtained is 0.9817 which is very close to 1 or considerably very high. It represents that actual value and predicted value are close enough which suggests it to be accurate. 98.17% of the total variation in wear can be associated with the experimental variables. Lack-of-fit value is 334.70 and probability of occurrence is almost 0%. The study reveals that the selected factors are appropriately produced and a relationship was established between the factors, by the obtained model. The P value for every coefficient was checked in order to evaluate the significance of the coefficient in the model. From Table 5, the F and P values obtained for the model developed for coefficient of friction are 44.67 and 0.000 respectively. The R^2 value for the model obtained is 0.9719 considerably high. The model had a lack-of-fit value of 14.22 and there is only 0.2% that is due to noise lack of fit of F value would occur.

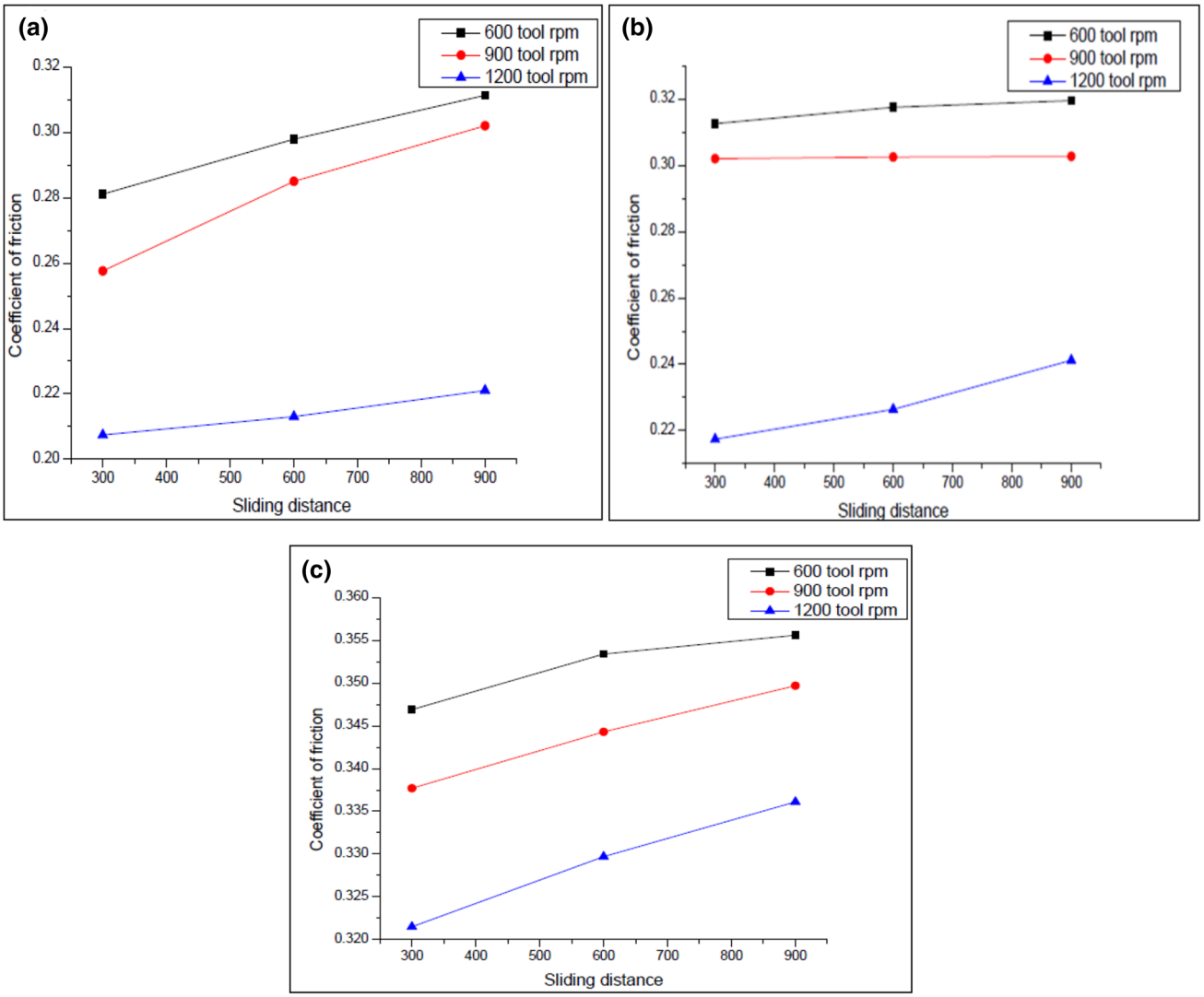

Fig. 5 Coefficient of friction versus Sliding distance at **a** 20 N applied load, **b** 30 N applied load, and **c** 40 N applied load

It represents that the obtained model is significant and complete, hence, producing a successful mathematical relationship between the factors.

The input variables are optimised by models developed for a minimum value of the coefficient of friction and minimum wear. Figure 6 shows the optimum values for input variables for the minimum coefficient of friction and wear. The optimized composite is to be fabricated at 1200 tool rpm and should be applied with a load of 20 N for a sliding distance of 300 m, to get a corresponding value of 24.483 for wear and 0.1805 for coefficient of friction as predicted by the model, same is shown in Table 6.

3.3 Analysis of Response Surface and Plots

Figures 7 and 8 shows the surface and counter plots of variation in wear and coefficient of friction with various input factors. The projection of the 3-D graph on the 2-D plot is shown by counter plots. Different ranges of wear loss are shown in different colours. As the colour of the counter plot turns from dark green to light green and then blue, wear and coefficient of friction value decrease correspondingly. So, it can be predicted that wear and coefficient of friction in minimum for the material fabricated at higher FSP tool rpm and which are slided for less distance and at low load.

3.4 ANN Modelling

Feed Forward Back Propagation is used to train the ANN model in MATLAB software. The designed data of 20 runs were divided into 15 (75% of data) and 5 (25% of data) data sets. 15 data sets were used for training and the remaining 5 for testing purpose. Graphical representation

Table 4 RSM ANOVA of regression equation results for wear

Source	DF	Adj SS	Adj MS	*F* value	*P* value
Model	9	21,460.2	2384.47	59.59	0.000
Linear	3	16,832.3	5610.78	140.22	0.000
X1	1	7920.1	7920.06	197.93	0.000
X2	1	3203.8	3203.76	80.07	0.000
X3	1	5708.5	5708.51	142.66	0.000
Square	3	1601.7	533.88	13.34	0.001
X1*X1	1	107.6	107.63	2.69	0.132
X2*X2	1	147.1	147.09	3.68	0.084
X3*X3	1	992.4	992.43	24.80	0.001
2-Way Interaction	3	3026.2	1008.74	25.21	0.000
X1*X2	1	581.9	581.94	14.54	0.003
X1*X3	1	2384.4	2384.37	59.59	0.000
X2*X3	1	59.9	59.92	1.50	0.249
Error	10	400.1	40.01		
Lack of Fit	3	397.4	132.46	334.70	0.000
Pure Error	7	2.8	0.40		

Table 5 RSM ANOVA of regression equation results for coefficient of friction

Source	DF	Adj SS	Adj MS	*F* value	*P* value
Model	9	0.026971	0.002997	38.40	0.000
Linear	3	0.022703	0.007568	96.96	0.000
X1	1	0.009821	0.009821	125.83	0.000
X2	1	0.000659	0.000659	8.44	0.016
X3	1	0.012223	0.012223	156.60	0.000
Square	3	0.003125	0.001042	13.34	0.001
X1*X1	1	0.001837	0.001837	23.53	0.001
X2*X2	1	0.000454	0.000454	5.82	0.037
X3*X3	1	0.001085	0.001085	13.90	0.004
2-Way Interaction	3	0.001144	0.000381	4.88	0.024
X1*X2	1	0.000071	0.000071	0.91	0.361
X1*X3	1	0.000992	0.000992	12.71	0.005
X2*X3	1	0.000080	0.000080	1.03	0.335
Error	10	0.000780	0.000078		
Lack of Fit	3	0.000670	0.000223	14.22	0.002
Pure error	7	0.000110	0.000016		

of the model is given in Fig. 9. The model consisted of 3 input factors that are tool rpm, sliding distance, and applied load, respectively, 10 hidden layers were decided on the basis of the literature studied [9, 43] and two outputs. Figure 10 shows the predictive performance curve for the developed model. Due to well training of model good coincidence is there between predicted and experimental values. Regression coefficient (*R*) showed a value

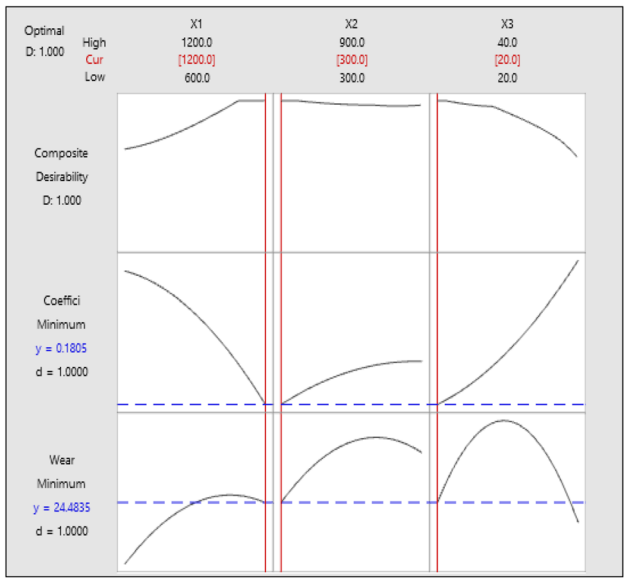

Fig. 6 Optimum results for minimum wear and coefficient of friction

Table 6 Solution of RSM optimization

Solution	X1	X2	X3	Coefficient of friction	Wear fit
1	1200	300	20	0.1805	24.4835

of 0.99996 which is close to 1 concludes that the model is of better quality.

3.5 RSM and ANN Predictive Capacity Evaluation

RSM and ANN along with %absolute error for both wear and coefficients of friction, respectively, are calculated using Eq. 3

$$\%absoluteerror = \frac{|Xexp - Xpre|}{Xexp} * 100 \quad (3)$$

Here, *X*exp is the experimental value and *X*pre is the predicted values by the model developed. In Table 7 predicted value for wear can be seen, it can be observed that %absolute error given by RSM and ANN model is 6.266 and 2.3595, respectively. In Table 8, values predicted by the developed models can be observed and %absolute error shown by the RSM model is 3.2979 and by ANN model is 1.8075. From both the tables, it can be concluded that values predicted by ANN are more accurate to experimental data compared to the values predicted by RSM. ANN model developed works better for analysing and prediction of data. Similar results were obtained when Karnik et al. did a comparative study of RSM and ANN modelling for burr size in drilling [45].

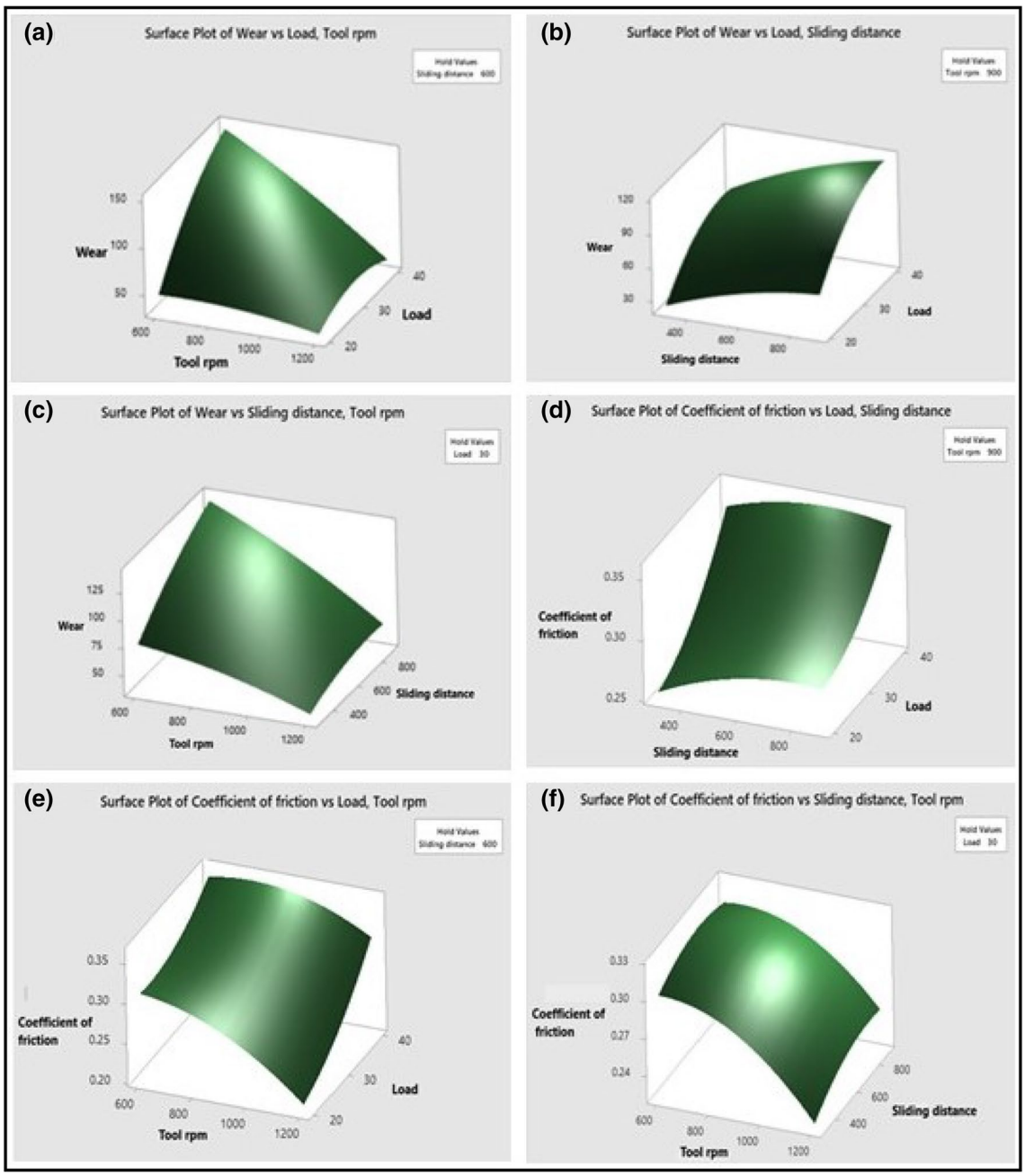

Fig. 7 Surface plot for **a** wear versus load, tool rpm **b** wear versus load, sliding distance **c** wear versus sliding distance, tool rpm **d** coefficient of friction vs load, sliding distance **e** coefficient of friction vs load, tool rpm **f** coefficient of friction vs sliding distance, tool rpm

3.6 Wear Morphology

Figure 11 shows SEM images of the fabricated composite. SEM analysis was done in order to find the effect of load and tool rpm on the tribological behaviour. Wear tracks can be seen in the above images. Traces of oxide tribo-layer formation can be seen in the SEM images of the worn surface. This might be responsible for the improved

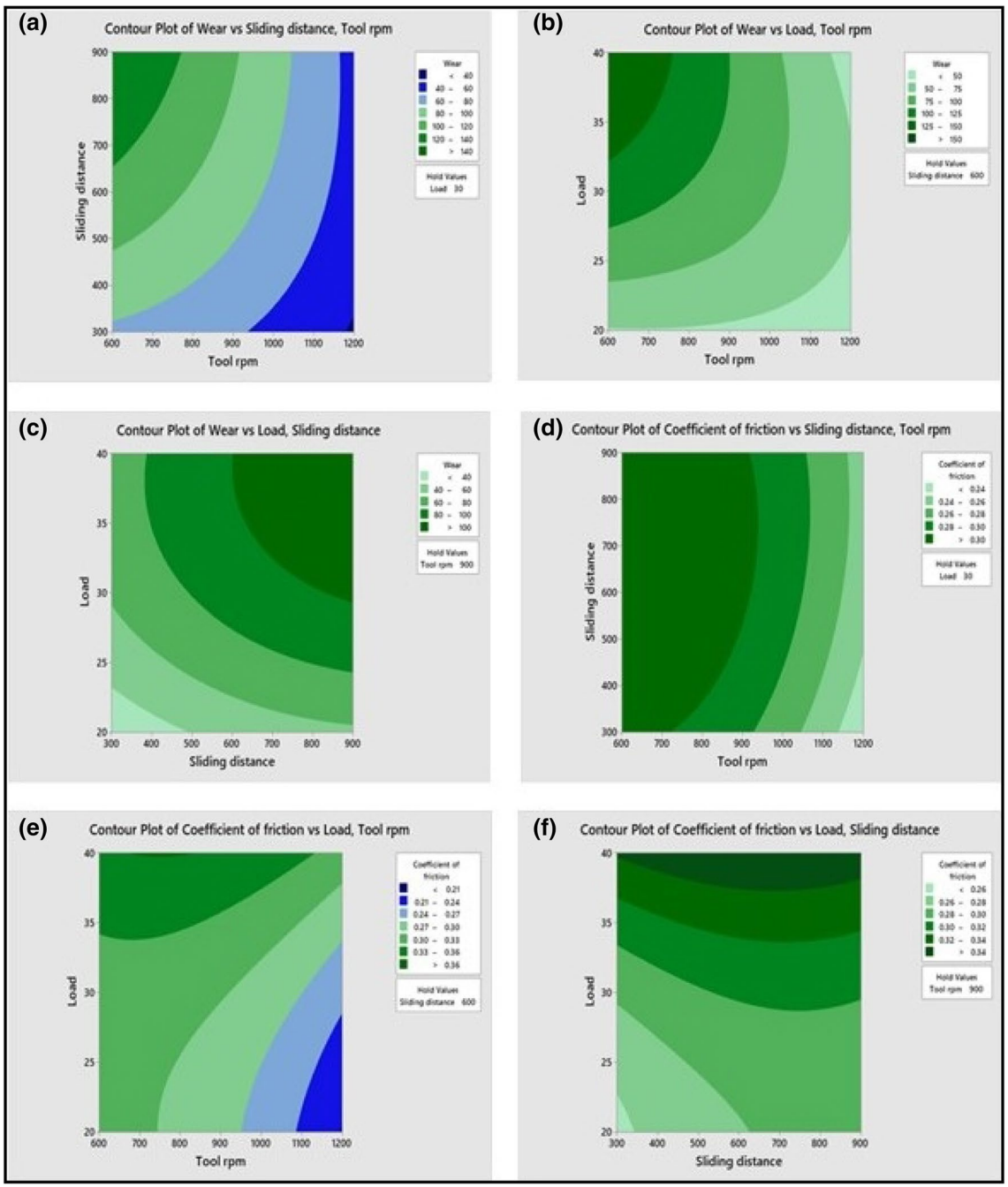

Fig. 8 Counter plot for **a** wear versus sliding distance, tool rpm **b** wear versus load, tool rpm **c** wear versus load, sliding distance **d** coefficient of friction versus sliding distance, tool rpm **e** coefficient of friction versus load, tool rpm **f** coefficient of friction vs load, sliding distance

tribological performance of the fabricated composite. Adhesion is seen in the images, reflecting that adhesive wear is the major wear mechanism taking place during the experiment. Figure 12 shows the elemental analysis of the fabricated composite samples. In Fig. 12, the presence of elements like C, O, Zn, Mg, Al, Si, and Fe is confirmed. The formation of oxide layer is confirmed with

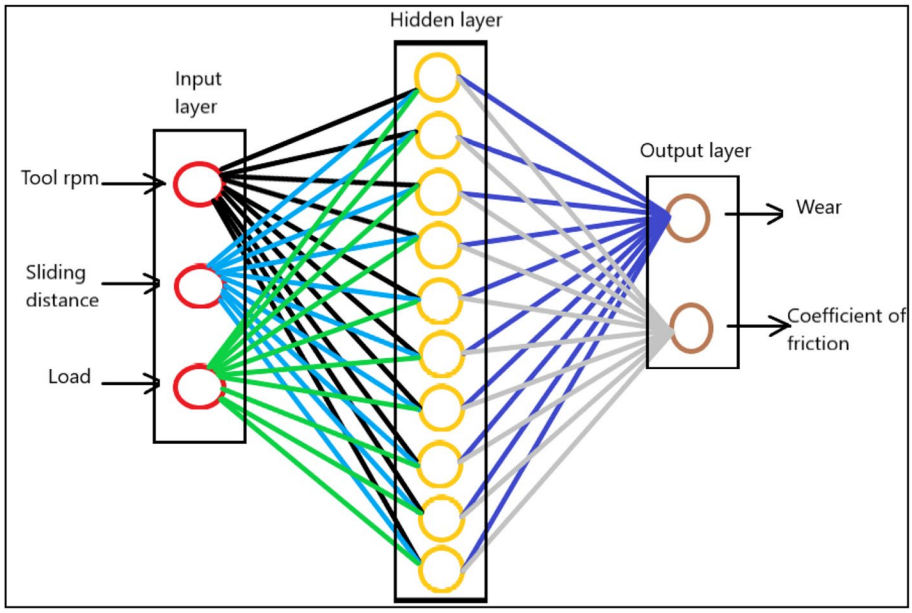

Fig. 9 Architectural representation of ANN model applied to the present study

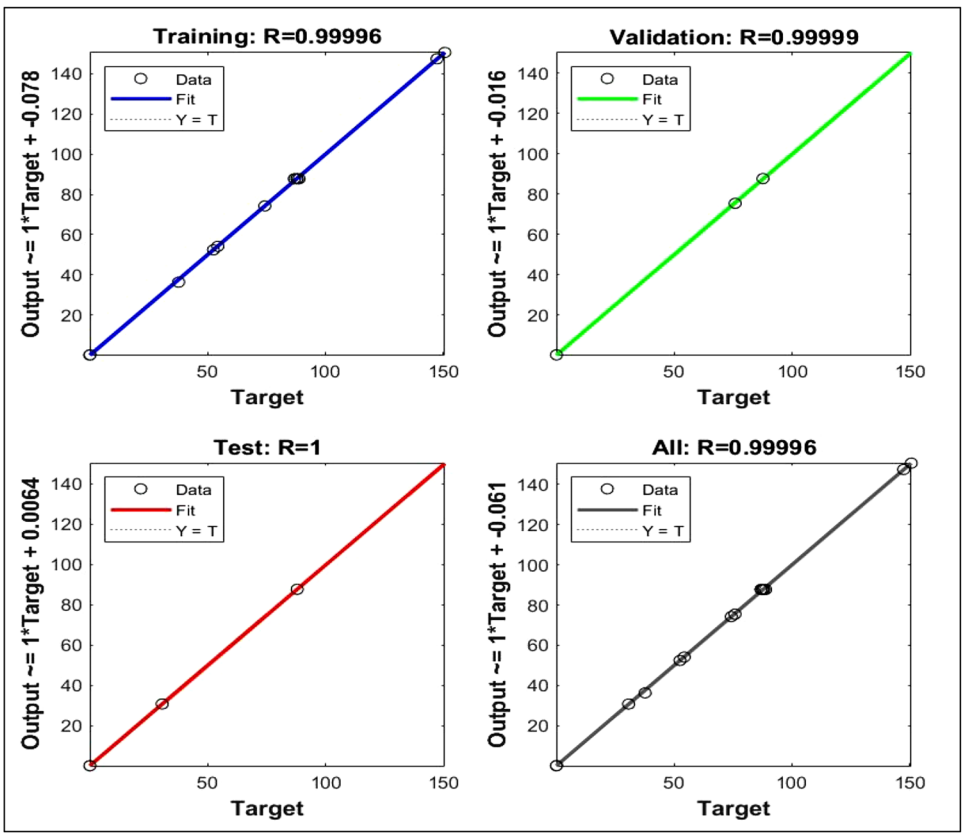

Fig. 10 Predictive performance curve for the present model

Table 7 Predictive responses by RSM and ANN for wear

Run	Experimental value	RSM value	ANN value	%absolute error in RSM values	%absolute error in ANN values
1	75.88	76.60763	75.4938	0.9589	0.5089
2	37.83	34.393	36.4083	9.0853	3.7581
3	74.33	70.16538	74.2517	5.6028	0.1053
4	87.001	87.74125	87.7618	0.8508	0.8744
5	52.599	56.76363	52.4869	7.9177	0.2131
6	88.056	87.74125	87.7618	0.3574	0.3341
7	147.31	150.747	147.3073	2.3331	0.0018
8	86.87	87.74125	87.7618	1.0029	1.0265
9	88.85	87.74125	87.7618	1.2478	1.2247
10	54.43	53.70238	54.1987	1.3368	0.4249
11	87.92	87.74125	87.7618	0.2033	0.1799
12	150.571	140.7546	150.4394	6.5194	0.0874
13	88.003	87.74125	87.7618	0.2974	0.2740
14	87.65	87.74125	87.7618	0.1041	0.1275
15	30.86	24.48063	30.868	20.6719	0.0259
16	87.58	87.74125	87.7618	0.1841	0.2075
17	111.55	117.9294	108.041	5.7188	3.1456
18	27.986	37.80238	31.0381	35.076	10.9058
19	44.64	38.98825	39.213	12.6607	12.1572
20	42.84	48.49175	47.8131	13.1927	11.6085
Average % absolute error				6.266	2.3595

Table 8 Predictive responses by RSM and ANN for coefficient of friction

Run	Experimental value	RSM value	ANN value	%absolute error in ANN values	%absolute error in RSM values
1	0.3126	0.31227	0.302863	0.1055	3.1148
2	0.213	0.21302	0.208175	0.0093	2.2652
3	0.3377	0.33122	0.342613	1.9188	1.4548
4	0.3012	0.30453	0.302688	1.1055	0.4940
5	0.2875	0.27206	0.282588	5.3704	1.7085
6	0.3025	0.30453	0.302688	0.6710	0.0621
7	0.3516	0.35156	0.356425	0.0113	1.3723
8	0.3073	0.30453	0.302688	0.9013	1.5008
9	0.31	0.30453	0.302688	1.7645	2.3587
10	0.2412	0.24799	0.250938	2.8150	4.0373
11	0.3022	0.30453	0.302688	0.7710	0.1614
12	0.3195	0.3241	0.312563	1.4397	2.1712
13	0.3001	0.30453	0.302688	1.4761	0.8623
14	0.2995	0.30453	0.302688	1.6794	1.0644
15	0.2576	0.21316	0.255488	17.2515	0.8198
16	0.2987	0.30453	0.302688	1.9517	1.3351
17	0.3497	0.35047	0.351813	0.2201	0.6042
18	0.2174	0.21338	0.224338	1.8491	3.1913
19	0.3297	0.26372	0.31785	20.0121	3.5941
20	0.2979	0.28409	0.30975	4.6357	3.9778
Average % absolute error				3.2979	1.8075

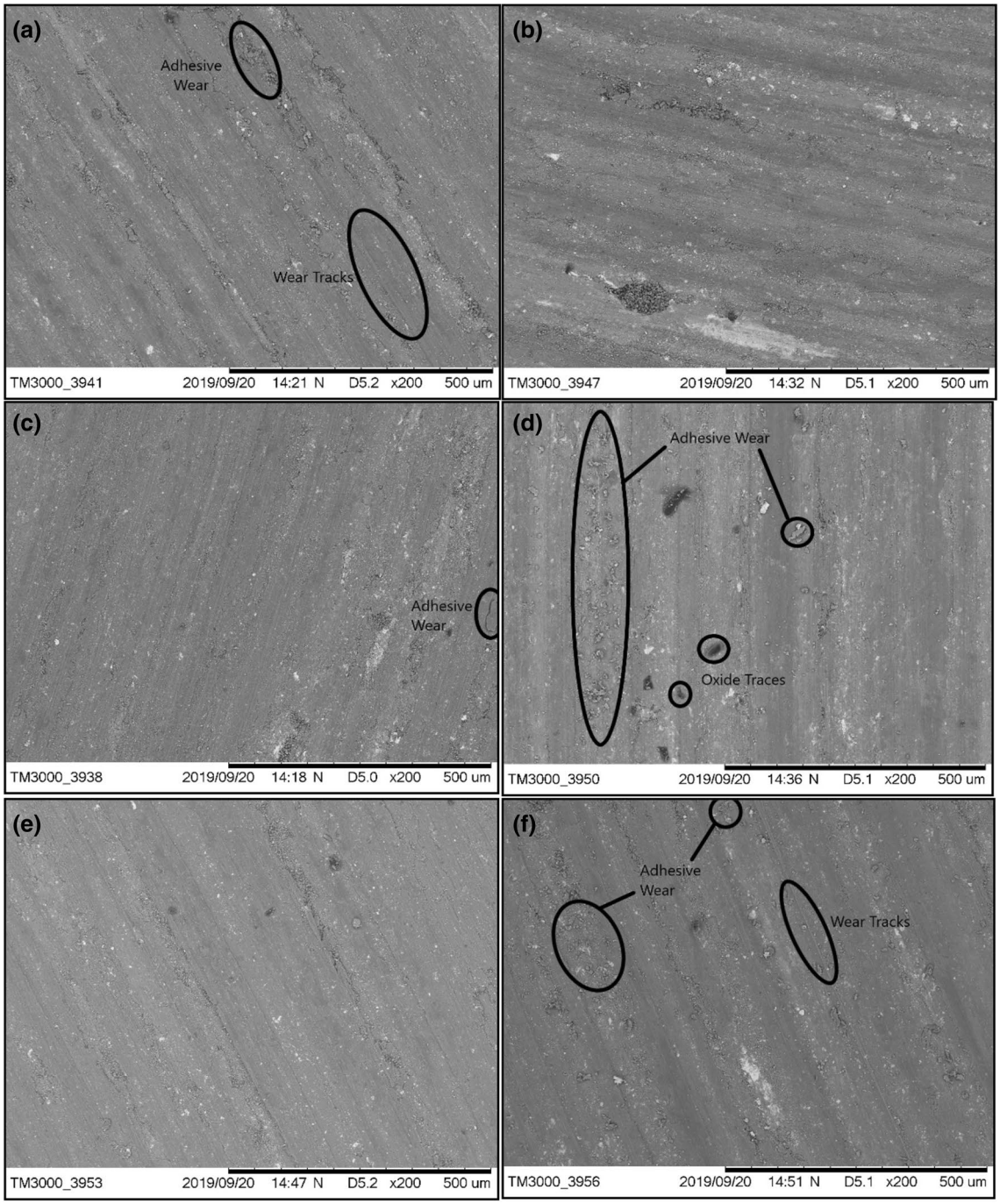

Fig. 11 Worn-out surface morphology images of samples fabricated at **a** 600 tool rpm applied with 20 N load, **b** 600 tool rpm applied with 40 N load, **c** 900 tool rpm applied with 20 N load, **d** 900 tool rpm applied with 40 N load, **e** 1200 tool rpm applied with 20 N load, and **f** 1200 tool rpm applied with 40 N load

the presence of oxygen in the analysis. When the wear pins slide on the disc, the surfaces get heated up and as a result reaction between oxygen and iron or aluminium takes place, initiating the formation of the tribo-oxide layer. Similar types of results are discussed in the study elsewhere [46–48].

4 Conclusion

1. With increasing applied load and sliding distance, both wear loss and coefficient of friction increases.

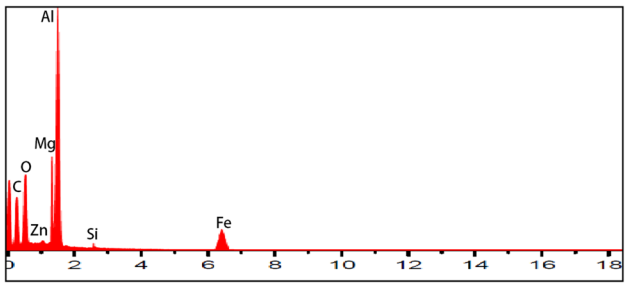

Fig. 12 EDS of fabricated composite sample

2. Wear resistance was enhanced for the fabricated surface composite at higher tool rotational speed.
3. Best wear resistance was shown by the surface composite fabricated at 1200 tool rotational speed (rpm) and sliding distance of 300 m at 20 N applied load.
4. Both response surface methodology (RSM) and artificial neural network (ANN) models were successfully developed.
5. ANN model best fitted the experimental values, concluding that ANN has a better predictive capacity.
6. Optimum experimental condition predicted by RSM is sliding distance of 300 m at an applied load of 20 N, for composite fabricated at 1200 tool rotational speed (rpm).
7. Scanning electron microscope (SEM) analysis of worn-out surface confirms that adhesive wear is the major wear mechanism.

Funding This work was supported by (TEQIP-III) Delhi Technological University.

Compliance with Ethical Standards

Conflict of interest The authors declare no conflicts of interest.

References

1. Butola R, Singari RM, Murtaza Q (2020) Mechanical and wear behaviour of friction stir processed surface composite through self-assembled monolayer technique. Surf Topogr 8(4):045007. https://doi.org/10.1088/2051-672X/abbcb8
2. Kumar G, Pramod R (2014) Artificial neural networks for predicting the tribological behaviour of Al7075-SiC metal matrix composites. Proc Int Conf Adv Eng Technol. https://doi.org/10.15224/978-1-63248-028-6-03-85
3. Kaufman JG (2002) Properties of aluminum alloys; tensile, creep, and fatigue data at high and low temperatures. ASM International, Cleveland
4. Butola R, Pratap C, Shukla A, Walia R (2019) Effect on the mechanical properties of aluminum-based hybrid metal matrix composite using stir casting method. Mater Sci Forum 969:253–259. https://doi.org/10.4028/www.scientific.net/msf.969.253
5. Butola R, Kanwar S, Tyagi L, Singari R, Tyagi M (2020) Optimizing the machining variables in CNC turning of aluminum based hybrid metal matrix composites. SN Applied Sciences, 2(8):1356. https://doi.org/10.1007/s42452-020-3155-8
6. Reddy M, Shakoor R, Parande G, Manakari V, Ubaid F, Mohamed A, Gupta M (2017) Enhanced performance of nano-sized SiC reinforced Al metal matrix nanocomposites synthesized through microwave sintering and hot extrusion techniques. Prog Nat Sci 27(5):606–614. https://doi.org/10.1016/j.pnsc.2017.08.015
7. Grover M, Sharma S, Kataria T, Samdani S, Agarwal S, Singh S (2018) Soft tissue reactions following cochlear implantation. Eur Arch Oto-Rhino-Laryngol 276(2):343–347. https://doi.org/10.1007/s00405-018-5233-8
8. Iqbal AA, Nuruzzaman DM (2016) Effect of the reinforcement on the mechanical properties of aluminium matrix composite: a review. Int J Appl Eng Res 11:10408
9. Kruk A, Mrózek M, Domagała J, Brylewski T, Gawlik W (2014) Synthesis and physicochemical properties of yttrium oxide doped with neodymium and lanthanum. J Electron Mater 43(9):3611–3617. https://doi.org/10.1007/s11664-014-3250-y
10. Butola R, Tyagi L, Singari R, Murtaza Q, Kumar H, Nayak D (2021) Mechanical and wear performance of Al/SiC surface composite prepared through friction stir processing. Materials Research Express. 8(1):016520https://doi.org/10.1088/2053-1591/abd89d
11. Alam M, Arif S, Ansari A (2019) Optimization of wear behaviour using Taguchi and ANN of fabricated aluminium matrix nanocomposites by two-step stir casting. Mater Res Express 6(6):065002. https://doi.org/10.1088/2053-1591/ab0871
12. Raghavendra N (2019) Wear studies on Al 7075/Al2O3 particulate MMC by Artificial Neural network. Int J Innov Res Sci Eng Technol 8(7)
13. Sha W, Edwards K (2007) The use of artificial neural networks in materials science based research. Mater Des 28(6):1747–1752. https://doi.org/10.1016/j.matdes.2007.02.009
14. Pramod R, Veeresh Kumar G, Gouda P, Mathew A (2018) A study on the Al2O3 reinforced Al7075 metal matrix composites wear behavior using artificial neural networks. Mater Today Proc 5(5):11376–11385. https://doi.org/10.1016/j.matpr.2018.02.105
15. Atrian A, Majzoobi G, Nourbakhsh S, Galehdari S, Masoudi Nejad R (2016) Evaluation of tensile strength of Al7075-SiC nanocomposite compacted by gas gun using spherical indentation test and neural networks. Adv Powder Technol 27(4):1821–1827. https://doi.org/10.1016/j.apt.2016.06.015
16. Mahanta S, Chandrasekaran M, Samanta S, Arunachalam R (2019) Multi-response ANN modelling and analysis on sliding wear behavior of Al7075/B4C/fly ash hybrid nanocomposites. Mater Res Express 6(8):0850h4. https://doi.org/10.1088/2053-1591/ab28d8
17. Kumar R, Dhiman S (2013) A study of sliding wear behaviors of Al-7075 alloy and Al-7075 hybrid composite by response surface methodology analysis. Mater Des 50:351–359. https://doi.org/10.1016/j.matdes.2013.02.038
18. Dehghani K, Nekahi A, Mirzaie M (2010) Optimizing the bake hardening behavior of Al7075 using response surface methodology. Mater Des 31(4):1768–1775. https://doi.org/10.1016/j.matdes.2009.11.014
19. Subramanian M, Sakthivel M, Sudhakaran R (2014) Modeling and analysis of surface roughness of AL7075-T6 in end milling process using response surface methodology. Arab J Sci Eng 39(10):7299–7313. https://doi.org/10.1007/s13369-014-1219-z
20. Sivasankaran S, Ramkumar K, Al-Mufadi F, Irfan O (2019) Effect of TiB2/Gr hybrid reinforcements in Al 7075 matrix on sliding wear behavior analyzed by response surface methodology. Met Mater Int. https://doi.org/10.1007/s12540-019-00543

21. Vishwakarma D, Kumar N, Padap A (2017) Modelling and optimization of aging parameters for thermal properties of Al 6082 alloy using response surface methodology. Mater Res Express 4(4):046502. https://doi.org/10.1088/2053-1591/aa68c1
22. Coyal A, Yuvaraj N, Butola R, Tyagi L (2020) An experimental analysis of tensile, hardness and wear properties of aluminium metal matrix composite through stir casting process. SN Appl Sci. https://doi.org/10.1007/s42452-020-2657-8
23. Parikh H, Gohil P (2017) Experimental investigation and prediction of wear behavior of cotton fiber polyester composites. Friction 5(2):183–193. https://doi.org/10.1007/s40544-017-0145-y
24. Abdelbary A, Abouelwafa M, El Fahham I (2014) Evaluation and prediction of the effect of load frequency on the wear properties of pre-cracked nylon 66. Friction 2(3):240–254. https://doi.org/10.1007/s40544-014-0044-4
25. Merayo D, Rodríguez-Prieto A, Camacho A (2020) Prediction of mechanical properties by artificial neural networks to characterize the plastic behavior of aluminum alloys. Materials 13(22):5227. https://doi.org/10.3390/ma13225227
26. Raj K, Sharma R, Singh P, Dayal A (2011) Study of friction stir processing (FSP) and high-pressure torsion (HPT) and their effect on mechanical properties. Procedia Eng 10:2904–2910. https://doi.org/10.1016/j.proeng.2011.04.482
27. Mouli D, Rao R, Kumar A (2017) A review on aluminium based metal matrix composites by friction stir processing. Int J Eng Manuf Sci 7(2):203–224
28. Gan Y, Solomon D, Reinbolt M (2010) Friction stir processing of particle reinforced composite materials. Materials 3(1):329–350. https://doi.org/10.3390/ma3010329
29. Chen T, Li L, Huang X (2005) Predicting the fibre diameter of melt blown nonwovens: comparison of physical, statistical and artificial neural network models. Modell Simul Mater Sci Eng 13(4):575–584. https://doi.org/10.1088/0965-0393/13/4/008
30. Butola R, Malhotra A, Yadav M, Singari RM, Murtaza Q, Chandra P (2019) Experimental studies on mechanical properties of metal matrix composites reinforced with natural fibres ashes. doi:https://doi.org/10.4271/2019-01-1123
31. Chaudhary A, Kumar Dev A, Goel A, Butola R, Ranganath M (2018) The Mechanical properties of different alloys in friction stir processing: a review. Mater Today Proc 5(2):5553–5562. https://doi.org/10.1016/j.matpr.2017.12.146
32. Butola R, Murtaza Q, Singari RM (2020) An experimental and simulation validation of residual stress measurement for manufacturing of friction stir processing tool. Indian J Eng Mater Sci 27(4):826–836
33. Butola R, Singari RM, Murtaza Q (2019) Fabrication and optimization of AA7075 matrix surface composites using Taguchi technique via friction stir processing (FSP). Eng Res Express 1(2):025015. https://doi.org/10.1088/2631-8695/ab4b00
34. Butola R, Murtaza Q, Singari R (2020) Formation of self-assembled monolayer and characterization of AA7075-T6/B4C nanoceramic surface composite using friction stir processing. Surf Topogr 8(2):025030. https://doi.org/10.1088/2051-672x/ab96db
35. Okewale A, Omoruwuo F, Adesina O (2019) Comparative studies of response surface methodology (RSM) and predictive capacity of artificial neural network (ANN) on mild steel corrosion inhibition using water hyacinth as an inhibitor. J Phys 1378:022002. https://doi.org/10.1088/1742-6596/1378/2/022002
36. Behera S, Meena H, Chakraborty S, Meikap B (2018) Application of response surface methodology (RSM) for optimization of leaching parameters for ash reduction from low-grade coal. Int J Min Sci Technol 28(4):621–629. https://doi.org/10.1016/j.ijmst.2018.04.014
37. Jiang Z, Zhang Z, Friedrich K (2007) Prediction on wear properties of polymer composites with artificial neural networks. Compos Sci Technol 67(2):168–176. https://doi.org/10.1016/j.compscitech.2006.07.026
38. Radhika N, Raghu R (2017) Investigation on mechanical properties and analysis of dry sliding wear behavior of Al LM13/AlN metal matrix composite based on Taguchi's technique. J Tribol. https://doi.org/10.1115/1.4035155
39. Haiter Lenin A, Vettivel S, Raja T, Belay L, Singh S (2018) A statistical prediction on wear and friction behavior of ZrC nano particles reinforced with Al Si composites using full factorial design. Surf Interfaces 10:149–161. https://doi.org/10.1016/j.surfin.2018.01.003
40. Radhika N, Raghu R (2017) Investigation on mechanical properties and analysis of dry sliding wear behavior of Al LM13/AlN metal matrix composite based on Taguchi's technique. J Tribol doi. https://doi.org/10.1115/1.4035155
41. Dorri Moghadam A, Omrani E, Menezes P, Rohatgi P (2015) Mechanical and tribological properties of self-lubricating metal matrix nanocomposites reinforced by carbon nanotubes (CNTs) and graphene – a review. Compos Part B Eng 77:402–420. https://doi.org/10.1016/j.compositesb.2015.03.014
42. Dama K, Prashanth L, Nagaral M, Mathapati R, Hanumantharayagouda M (2017) Microstructure and mechanical behavior of B4C particulates reinforced ZA27 alloy composites. Mater Today Proc 4(8):7546–7553. https://doi.org/10.1016/j.matpr.2017.07.086
43. Shaikh M, Raja S, Ahmed M, Zubair M, Khan A, Ali M (2019) Rice husk ash reinforced aluminium matrix composites: fabrication, characterization, statistical analysis and artificial neural network modelling. Mater Res Express 6(5):056518. https://doi.org/10.1088/2053-1591/aafbe2
44. Raaft M, Mahmoud T, Zakaria H, Khalifa T (2011) Microstructural, mechanical and wear behavior of A390/graphite and A390/Al2O3 surface composites fabricated using FSP. Mater Sci Eng A 528(18):5741–5746. https://doi.org/10.1016/j.msea.2011.03.097
45. Karnik S, Gaitonde V, Davim J (2007) A comparative study of the ANN and RSM modelling approaches for predicting burr size in drilling. Int J Adv Manuf Technol 38(9–10):868–883. https://doi.org/10.1007/s00170-007-1140-7
46. Alam M, Arif S, Ansari A (2018) Wear behaviour and morphology of stir cast aluminium/SiC nanocomposites. Mater Res Express 5(4):045008. https://doi.org/10.1088/2053-1591/aab7b3
47. Tyagi L, Butola R, Jha A (2020) Mechanical and tribological properties of AA7075-T6 metal matrix composite reinforced with ceramic particles and aloevera ash via Friction stir processing. Mater Res Express 7(6):066526. https://doi.org/10.1088/2053-1591/ab9c5e
48. Butola R, Tyagi L, Kem L, Singari RM, Murtaza Q (2020) Mechanical and wear properties of aluminium alloy composites: a review. Lecture notes on multidisciplinary industrial engineering. Springer, Singapore